

University of Windsor

## Scholarship at UWindsor

---

Electronic Theses and Dissertations

Theses, Dissertations, and Major Papers

---

1-1-1965

### A triple cavity ammonia maser.

J. W. L. Hastings  
*University of Windsor*

Follow this and additional works at: <https://scholar.uwindsor.ca/etd>

---

#### Recommended Citation

Hastings, J. W. L., "A triple cavity ammonia maser." (1965). *Electronic Theses and Dissertations*. 6386.  
<https://scholar.uwindsor.ca/etd/6386>

This online database contains the full-text of PhD dissertations and Masters' theses of University of Windsor students from 1954 forward. These documents are made available for personal study and research purposes only, in accordance with the Canadian Copyright Act and the Creative Commons license—CC BY-NC-ND (Attribution, Non-Commercial, No Derivative Works). Under this license, works must always be attributed to the copyright holder (original author), cannot be used for any commercial purposes, and may not be altered. Any other use would require the permission of the copyright holder. Students may inquire about withdrawing their dissertation and/or thesis from this database. For additional inquiries, please contact the repository administrator via email ([scholarship@uwindsor.ca](mailto:scholarship@uwindsor.ca)) or by telephone at 519-253-3000ext. 3208.

A TRIPLE CAVITY AMMONIA MASER

BY

J. W. L. HASTINGS

A Thesis

Submitted to the Faculty of Graduate Studies through the  
Department of Physics in Partial Fulfillment  
of the Requirements for the Degree of  
Master of Science at  
the  
University of Windsor

Windsor, Ontario

1965

UMI Number: EC52567

### INFORMATION TO USERS

The quality of this reproduction is dependent upon the quality of the copy submitted. Broken or indistinct print, colored or poor quality illustrations and photographs, print bleed-through, substandard margins, and improper alignment can adversely affect reproduction.

In the unlikely event that the author did not send a complete manuscript and there are missing pages, these will be noted. Also, if unauthorized copyright material had to be removed, a note will indicate the deletion.

**UMI**<sup>®</sup>

---

UMI Microform EC52567

Copyright 2008 by ProQuest LLC.

All rights reserved. This microform edition is protected against unauthorized copying under Title 17, United States Code.

ProQuest LLC  
789 E. Eisenhower Parkway  
PO Box 1346  
Ann Arbor, MI 48106-1346

APPROVED:

..... S. N. Kalra .....

S. N. Kalra

..... A. van Wijngaarden .....

A. van Wijngaarden

..... F. Holuj .....

F. Holuj (Supervisor)

120924

## ABSTRACT

The line shape of an ammonia maser, based on the principle of Ramsey separated oscillatory fields, has been investigated with a cavity system employing a TE mode of oscillation. Two plausible explanations are given for the line shape observed although no positive conclusions are reached.

## PREFACE

In 1954 Gordon, Zeiger and Townes<sup>(9)</sup> obtained oscillations in the microwave region through the stimulated emission of radiation, from the ammonia molecule. Since that time many attempts have been made to apply the narrow lines in the inversion spectrum of ammonia to use as frequency standards. In the maser the width of the emission line depends upon the time of interaction, of the ammonia beam, with the field that stimulates the emission. In 1962, Holuj, Kalra and Daams<sup>(7)</sup> succeeded in reducing the line width by using a cavity system, oscillating in a TM mode, which produced the effects of Ramsey separated oscillating fields. In this experiment a similar system was used, employing a TE mode of oscillation.

In the following the necessary theory, for the understanding of the ammonia maser, is first developed, then the details and the results of the experiment are given.

#### ACKNOWLEDGEMENTS

I should like to express my gratitude to Dr. Frank Holuj for his able supervision and to Mr. W. Grewe for his assistance in overcoming the mechanical problems involved in this experiment.

I wish also to acknowledge the financial aid extended to me by the Province of Ontario, in the form of a bursary.

## TABLE OF CONTENTS

ABSTRACT	ii
PREFACE	iii
ACKNOWLEDGEMENTS	iv
LIST OF FIGURES	vi
CHAPTER I - THEORY OF THE AMMONIA MOLECULE	
Rotational Spectrum of Ammonia	1
Inversion Spectrum of Ammonia	2
Hyperfine Structure in the Inversion Spectrum of Ammonia	8
CHAPTER II - AN AMMONIA BEAM AS A TWO LEVEL SYSTEM	
Stationary States of an Ammonia Beam	12
An Ammonia Beam in an Electric Field	13
An Ammonia Beam in a Time Dependent Electric Field	16
An Ammonia Beam in Separated Oscillating Electric Fields	17
CHAPTER III - THEORY OF THE AMMONIA MASER	21
CHAPTER IV - APPARATUS	
Introduction	27
Sources	27
State Selectors	29
Cavity System	29
Electronics	33
Vacuum System	36
CHAPTER V - EXPERIMENTATION AND RESULTS	37
CHAPTER VI - DISCUSSION	41
REFERENCES	44
VITA AUTORIS	45



## LIST OF FIGURES

Figure	Page
1. Ammonia molecule.	3
2. Rotational energy levels of ammonia.	3
3. Potential experienced by nitrogen in ammonia.	4
4. Parabolic potential with barrier.	6
5. Ammonia coupling scheme, hyperfine energy levels, and relative intensities of hyperfine components.	10
6. Transition probability curves.	19
7. TE cavity system.	23
8. Superimposed Ramsey transition probabilities, for hyperfine components.	26
9. Outline of apparatus.	28
10. State selectors.	30
11. Cavity frequency measurement.	32
12. Block diagram of electronics.	34
13. Line shape of ammonia maser.	39
14. Line shape with and without shutter.	40

CHAPTER I  
THEORY OF THE AMMONIA MOLECULE

Rotational Spectrum of Ammonia

The  $\text{NH}_3$  molecule is a symmetric top. It is in the form of a pyramid whose base is formed by the three hydrogen atoms, and whose apex is formed by the nitrogen atom. The three hydrogen atoms form an equilateral triangle and the distance between the Nitrogen and each of the Hydrogens is the same.

Rotations of this molecule can be described as follows. The molecular or  $z$  axis is chosen as shown in Figure (1). This axis is a three-fold axis of symmetry. The moment of inertia about the  $z$  axis is usually denoted by  $I_A$  and the moment of inertia about any axis normal to the  $z$  axis is denoted  $I_B$ . Where the  $x$  and  $y$  axes are chosen arbitrarily. If the molecule has an angular momentum,  $\vec{P}$ , in an arbitrary direction, the rotational energy is given by;

$$W = \frac{p^2}{2I_B} + \frac{P_z^2}{2I_A} \left( \frac{1}{2I_A} - \frac{1}{2I_B} \right) \quad (1)$$

According to Quantum Mechanics  $P$  must be replaced by

$$\sqrt{J(J+1)}\hbar$$

where  $J$  is the angular momentum quantum number, and its projection in the  $z$  direction,  $P_z$ , is replaced by;  $\hbar K$  where  $K$  assumes values

Eq. (1) can be written:

$$W = \frac{J(J+1)h^2}{8\pi^2 I_B} + \left( \frac{h^2}{8\pi^2 I_A} - \frac{h^2}{8\pi^2 I_B} \right) K^2 \quad (2)$$

Substituting  $A = \frac{h^2}{2I_A}$ ,  $B = \frac{h^2}{2I_B}$  into Eq. (2) yields,

$$W = BJ(J+1) + (A - B)K^2 \quad (3)$$

For ammonia the values of A and B are, (1)

$$A = 189 \times 10^{13} \text{mc.}^2, \quad B = 298 \times 10^{13} \text{mc.}^2$$

The expected rotational energy levels are shown in Fig. (2)

For a transition between levels with different J values, a selection rule  $\Delta K = 0$  is rigorously obeyed because the resultant dipole moment is along the z axis. For a dipole transition, the selection rule  $\Delta J = 0, \pm 1$  holds, hence the frequencies of the rotational spectra are given by;

$$\nu = 2B(J+1).$$

#### Inversion Spectrum of Ammonia

The energy levels between which the maser action occurs, are those due to inversion. The ammonia molecule can be found with the nitrogen on either side of the plane formed by the hydrogens. The potential acting on the nitrogen atom, in ammonia, along the symmetry axis is plotted in Figure (3a), as a function of s, the distance from the plane formed by the hydrogen atoms. (1)  
Fig. (3b) shows the vibrational energy levels of the nitrogen atom.

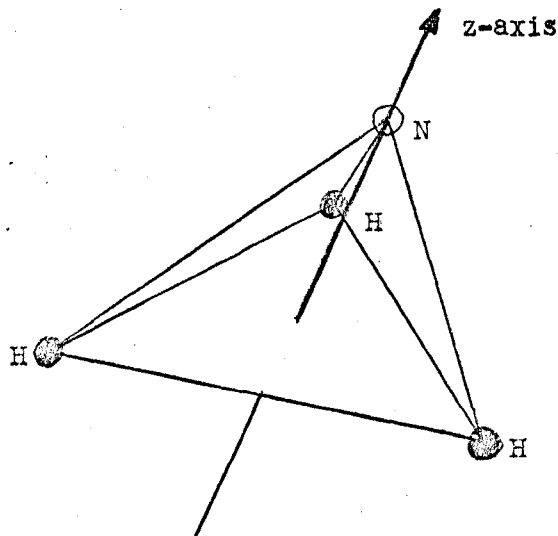


Figure (1). The ammonia molecule with molecular (z) axis indicated.

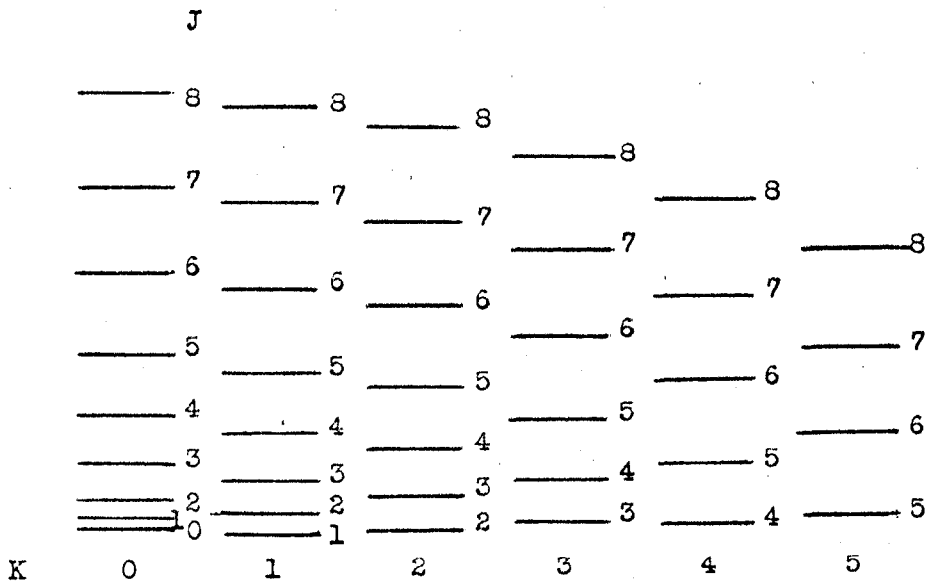


Figure (2). Rotational energy levels denoted by quantum numbers J and K.

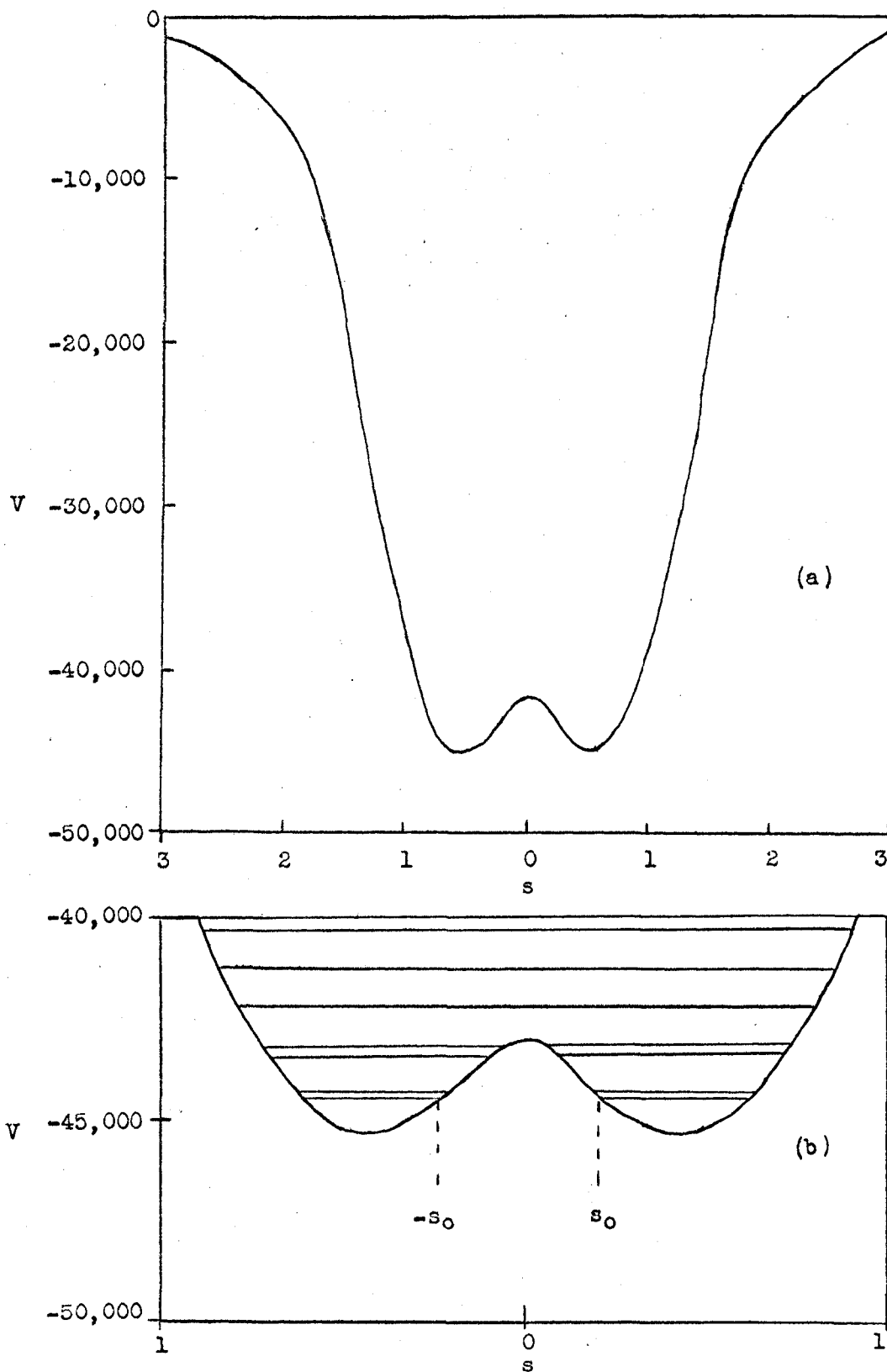


Fig. (3). Potential energy for nitrogen along  $z$ -axis of ammonia where  $s$  represents the distance from the hydrogen plane and  $V$  the potential in  $1/\text{cm}$ . (b) shows the vibrational energy levels in the lower portion of curve (a).

The lower levels are doubled, as will be explained below, and it is between the two levels of these doubled levels that the inversion transitions occur.

The inversion transitions can be understood qualitatively as follows. Consider an atom in the potential depicted in Fig. (4a). The vibrational energy levels are evenly spaced, the spacings corresponding to transitions in the infrared. Townes has shown that for even  $K$  the ground state vibrational wave function is even while that of the first excited state is odd. The reverse is true for  $K$  odd.<sup>(1)</sup> These wave functions are shown in Fig. (4b). Upon the introduction of a potential barrier, the wave functions retain their symmetry, but the energy levels are modified. This situation is illustrated in Fig. 4 (c) and (d). In ammonia the energy difference between the two lowest vibrational energy levels is in the microwave region. Transitions between these two levels are referred to as inversion transitions.

If the wave functions corresponding to the first two vibrational energy levels are  $\Psi_I$  and  $\Psi_{II}$  and the energies associated with them are  $W_I$  and  $W_I + \Delta$ , respectively the time dependence of the wave functions is given by

$$\Psi_I e^{i W_I t / \hbar} \quad \Psi_{II} e^{i (W_I + \Delta) t / \hbar}$$

Let the wave function corresponding to the lowest state of simple harmonic oscillation with the nitrogen to the left be denoted by  $U_L$ , and that for the nitrogen on the right by  $U_R$ . The true

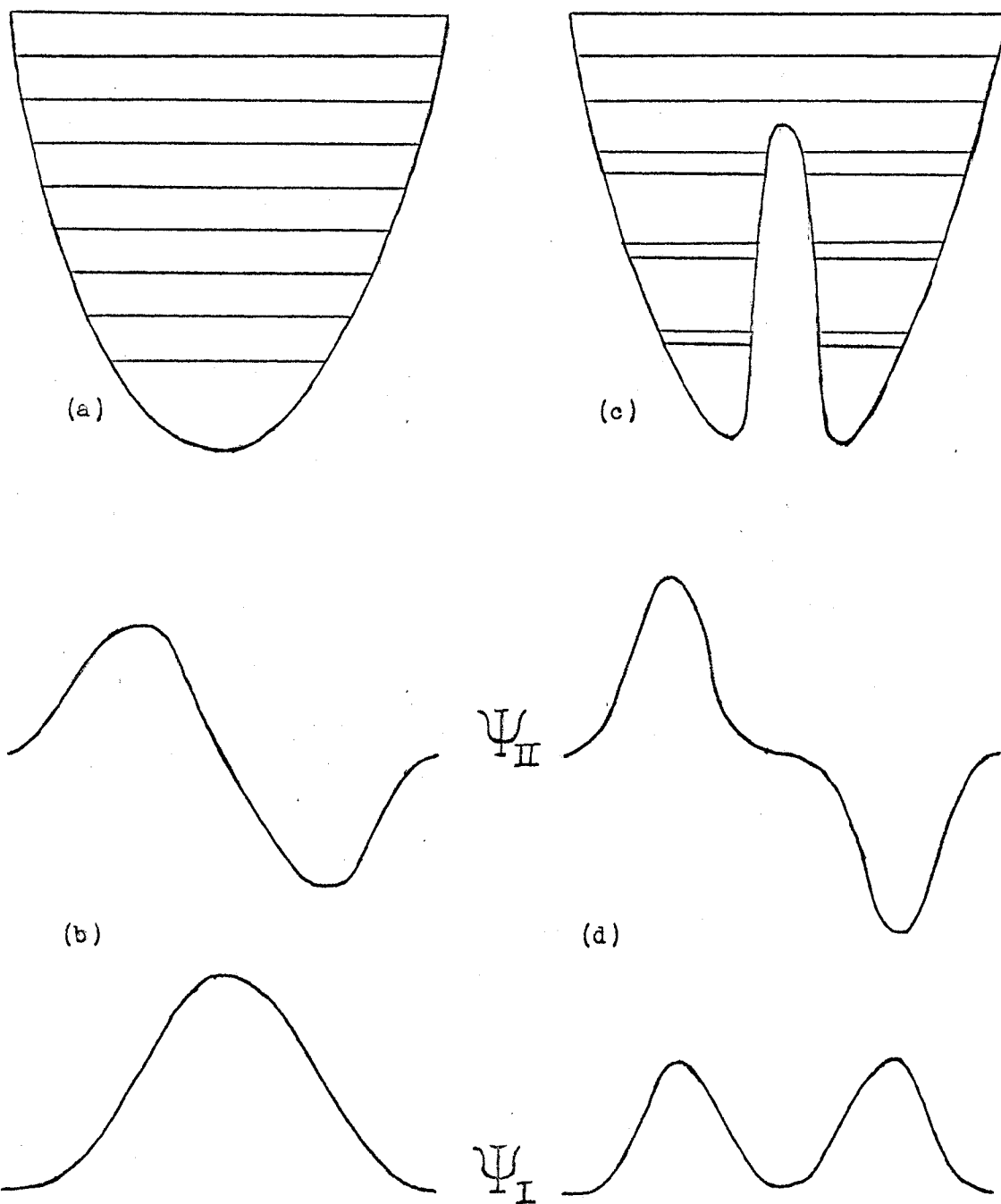


Fig. (4). (a) Parabolic potential well with vibrational energy levels indicated. (b) Wave functions for the two lowest energy levels in the potential of (a). (c) Change of vibrational energy levels when a potential barrier modifies a parabolic potential well. (d) Wave functions for modified potential well.

molecular wave functions, which have a definite energy, must be either symmetric or anti-symmetric with respect to inversion. Thus the wave functions corresponding to the upper and lower levels of the lowest vibrational doublet must be:

$$\begin{aligned}\Psi_{II} &= \frac{1}{\sqrt{2}} (U_L - U_R) \\ \Psi_I &= \frac{1}{\sqrt{2}} (U_L + U_R) .\end{aligned}\tag{4}$$

If at time  $t = 0$  the nitrogen is found on the left side, then the wave function is,

$$\Psi = \frac{1}{\sqrt{2}} (\Psi_I + \Psi_{II}) = U_L.$$

At some time,  $t$ , later, the wave function becomes:

$$\Psi = \frac{1}{\sqrt{2}} (\Psi_I + \Psi_{II} e^{i\omega_0 t}) e^{iW_I t/\hbar},$$

which at a time  $t = \frac{2\pi}{\omega_0}$  becomes:

$$\Psi = \frac{1}{\sqrt{2}} (\Psi_I - \Psi_{II}) e^{iW_I t/\hbar} = U_R e^{iW_I t/\hbar}.$$

Hence the nitrogen has moved to the right side. For a time

$t \ll \frac{2\pi}{\omega_0}$ ,  $\Psi$  may be expanded to yield,

$$\begin{aligned}\Psi &= \frac{1}{\sqrt{2}} \left\{ (\Psi_I + \Psi_{II}) + \frac{i\omega_0 t}{\sqrt{2}} \Psi_{II} \right\} e^{iW_I t/\hbar} \\ &= U_L + \frac{i\omega_0 t}{2} (U_L - U_R) .\end{aligned}\tag{5}$$

Thus the amplitude of the wave function on the right has grown by



a factor of:

$$\frac{\omega_0 t}{2} \quad (6)$$

This measures the rate at which the wave function penetrates the potential barrier in terms of  $\omega_0$ .

The penetration can be related to the vibrational frequency,  $\omega_v$ , in the following manner. An approximate solution to Schrodinger's equation in the region of the boundary yields the expression, (1)

$$\begin{aligned} \Psi_{I}(s = s_0) &= \exp \frac{i}{\hbar} \int_{-s_0}^s 2K(V(s) - W_I) ds \\ &= \frac{1}{A^2} \end{aligned}$$

which denotes the amplitude transmitted through the barrier when the nitrogen strikes it. In a time  $t$  the nitrogen strikes the barrier  $\frac{\omega_v t}{2}$  times, transmitting an amplitude  $\frac{\omega_v t}{2\pi A^2}$ . This may be equated to expression (6) to yield the inversion frequency:

$$\omega_0 = \frac{\omega_v}{\pi A^2}$$

#### Hyperfine Structure in the Inversion Spectrum of Ammonia

In the preceding analysis the hyperfine structure of the inversion levels due to the spin of the nitrogen and hydrogen nuclei was neglected. The effect of this coupling between the

nuclear spin of the nitrogen atom,  $I_N$ , and the angular momentum  $J$  must be considered. Of these the most important is the electric quadrupole coupling term<sup>(2)</sup>:

$$W_{JKF_1} = -\langle v | eQq | v \rangle \frac{(1 - 3K^2)}{J(J+1)} \Omega_1(\vec{J}, \vec{I}_N), \quad (7)$$

$$\Omega_1(\vec{J}, \vec{I}_N) = \frac{3(\vec{I}_N \cdot \vec{J})^2 + \frac{3}{2}(\vec{I}_N \cdot \vec{J}) - I_N(I_N + 1) J(J+1)}{2(J-1)(2J+3) 2I_N(2I_N-1)}.$$

Fig. (5a) shows the zero field coupling scheme for the ammonia molecule, in which the spins of the hydrogens have been included. The quantum number denoting the resultant of the coupling between  $J$  and  $I_N$  is  $F_1 = J + I_N$ . Let us now consider a system composed of molecules in the  $J = K = 3$  inversion state. For such molecules  $F_1$  takes on the values 2, 3, and 4. It has been shown by Gordon<sup>(2)</sup> that the quadrupole coupling constant,  $eQq$ , is approximately 4kc/sec. higher in the lower inversion state than in upper. The result of this is that  $\Delta F_1 = 0$  transitions which occur between the upper and lower inversion states with  $J = K = 3$  and with  $F_1 = 2, 3, \text{ or } 4$ , have different frequencies. Figure (5c) shows the difference in frequency that results for these transitions, compared to the frequency that would occur if the quadrupole coupling constant were the same for both inversion states. The relative number in each state is also indicated in this figure.

If the ammonia molecule is placed in a region of high electric field,  $F_1$  is no longer a good quantum number. In the

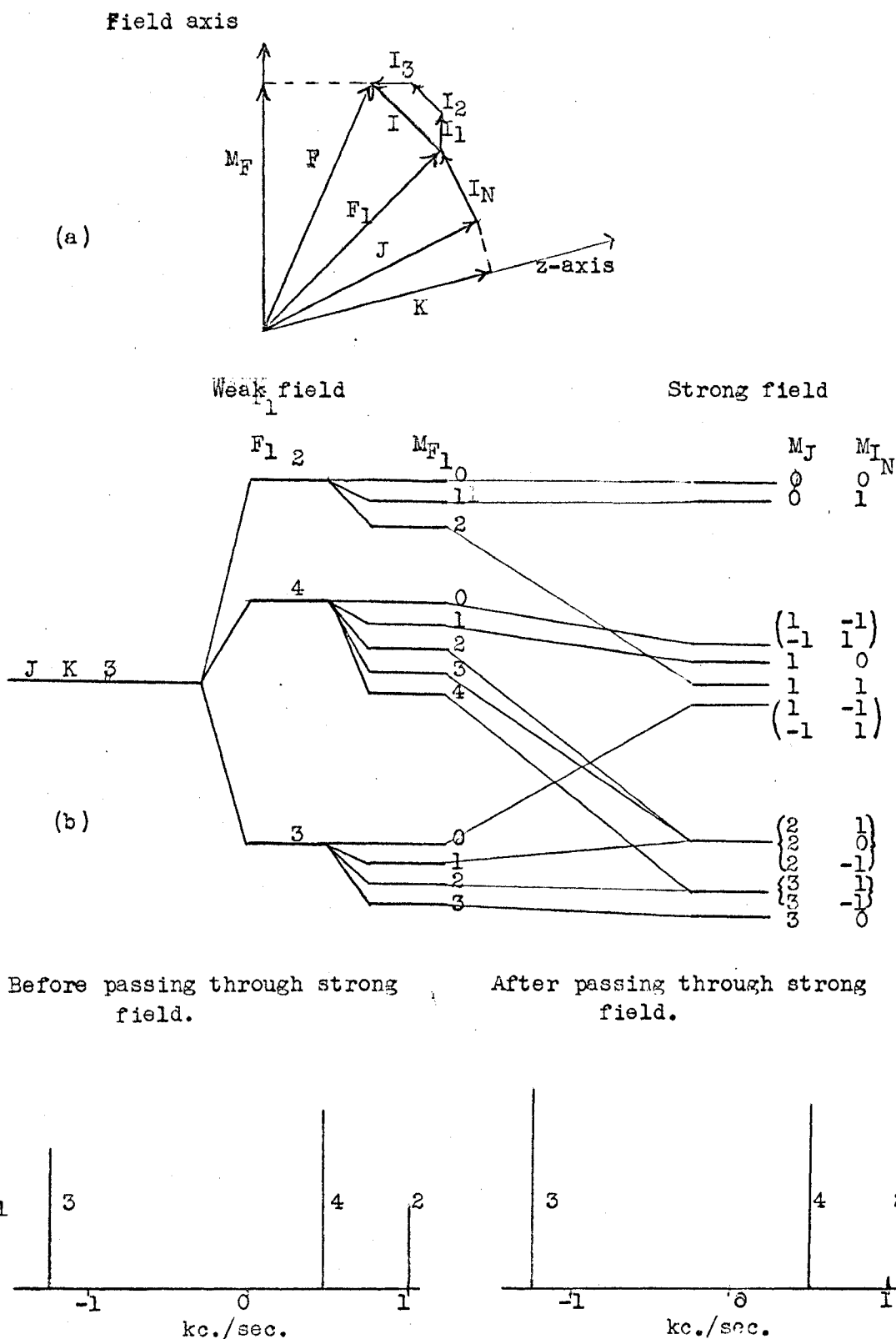


Fig. (5). (a) Weak field coupling scheme. (b) Weak and strong field energy levels, neglecting hydrogen spins.<sup>(9)</sup> (c) Relative intensities and frequencies of hyperfine components, before and after passing through strong field.<sup>(3)</sup>

high field case  $J$  and  $I_N$  decouple. Figure (5b) indicates which low field states go to which high field states during an adiabatic transition between the two cases.

## CHAPTER II

### AN AMMONIA BEAM AS A TWO LEVEL SYSTEM

The maser studied was of the two level type. The following will show how a favourable two level system can be obtained, using the inversion states of ammonia.

#### Stationary States

Consider the two eigenfunctions  $U_L$  and  $U_R$  as basis eigenfunctions used to form the two wave functions  $\Psi_I$  and  $\Psi_{II}$  which describe the ground and excited states of the two level system. The Hamiltonian,  $H$ , has for eigenfunctions the two states  $\Psi_I$  and  $\Psi_{II}$ . The matrix of this Hamiltonian may be formed between the two states  $U_L, U_R$ . Let:

$$\langle U_R | H | U_R \rangle = \langle U_L | H | U_L \rangle = E_0 \quad ,$$

which is true because there is no physical reason for the energy to depend on whether the nitrogen is on the left or on the right, and

$$\langle U_R | H | U_L \rangle = \langle U_L | H | U_R \rangle^* = -A \quad .$$

where  $-A$  represents the possibility that the nitrogen can tunnel from the left to the right.

The secular determinant, 
$$\begin{vmatrix} E_0 - W & -A \\ -A & E_0 - W \end{vmatrix} = 0$$

yields the eigenvalues of  $H$  :

$$W_{I,II} = E_0 \mp A, \quad (8)$$

and the eigenfunctions:

$$\Psi_{I,II} = \frac{1}{\sqrt{2}} (U_L \pm U_R)$$

The beam consists of a mixture of molecules in the states  $\Psi_I$  and  $\Psi_{II}$ . The wave function describing the beam is written:

$$\Psi = c_I \Psi_I + c_{II} \Psi_{II},$$

where  $|c_I|^2$  and  $|c_{II}|^2$  are the probability amplitudes.

#### An Ammonia Beam In an Electric Field

If an ammonia molecule is placed in an electric field  $\vec{E}$ , the energy of the molecule is changed by an amount  $-\vec{\mu} \cdot \vec{E}$ , where  $\vec{\mu}$  is the dipole moment of the molecule. Supposing that the electric field is pointing from right to left, the matrix elements of  $H^1$  may be written between the bases  $U_L, U_R$ , to yield,

$$\begin{aligned} \langle U_R | H^1 | U_R \rangle &= E_0 + uE \\ \langle U_L | H^1 | U_L \rangle &= E_0 - uE \\ \langle U_R | H^1 | U_L \rangle &= \langle U_L | H^1 | U_R \rangle^* = -A, \end{aligned} \quad (10)$$

where  $u$  is the magnitude of the dipole moment in the direction of the field, and  $E$  is the magnitude of the field. The secular determinant becomes

$$\begin{vmatrix} E_0 + uE - W & -A \\ -A & E_0 - uE - W \end{vmatrix} = 0,$$

which yields the energy eigenvalues :

$$W_{I,II} = E_0 \pm \sqrt{A^2 + (uE)^2}, \quad (11)$$

corresponding to the eigenfunctions:

$$\Psi_{I,II} = \frac{1}{\sqrt{2}} (U_L \pm U_R).$$

Hence the energy of the upper state,  $\Psi_{II}$ , increases with the square of the electric field while that of the lower state,  $\Psi_I$ , decreases. For experimentally achievable fields  $uE \ll A$  and Eq.(11) may be expanded to give:

$$\begin{aligned} W_I &= E_0 - A - \frac{(uE)^2}{2A} \\ W_{II} &= E_0 + A + \frac{(uE)^2}{2A}. \end{aligned} \quad (12)$$

If a beam of ammonia molecules is passed through an electric field in which  $E$  increases radially from the centre of the beam, the lower state molecules will move to the region of lowest energy and be removed from the beam. The upper state molecules will also move to the region of lowest energy, which is at the centre of the beam.

The quantity  $uE$  can be written in terms of the rotational quantum numbers  $J$ ,  $K$  and  $M$ , where  $M$  is the quantum number for the projection of the rotational angular momentum on the field. The

dipole moment of the ammonia molecule points in the direction of the molecular axis. If  $\vec{P}$  is the angular momentum of the molecule, the component of the dipole moment in the direction of  $\vec{P}$  is given by  $\mu K/J(J+1)$  where  $K$  and  $J$  have the same definitions as before.

Writing the angle between  $\vec{P}$  and  $\vec{E}$  in terms of  $M$  and  $J$  the expression,

$$\mu E = |\mu||E| MK/J(J+1), \quad (13)$$

is obtained. It follows from Equation (12) that the force exerted by an electric field on an ammonia molecule with a given  $J$  and  $K$ , depends on the value of  $M^2$ .

Passage of an ammonia beam through a strong electric field changes the relative populations of the hyperfine energy states denoted by  $F_1$ . Consider ammonia molecules in the  $J = 3$  and  $K = 3$  state initially in thermodynamic equilibrium. The relative populations of the  $F_1 = 2, 3$  and 4 levels is 5:7:9. When the molecules enter the field, designed to remove those in the lower state and focus those in the upper state  $I_N$  and  $J$  are decoupled and the weak field states change to strong field states as is shown in Figure (5b). In the strong field the force exerted on the molecules depends on  $M^2$ . Thus the relative number of the weak field states after the molecules have been passed through a strong field depends on  $\sum M^2$ . Where the summation is carried out over the values of  $M$  that a particular  $F_1$  takes on when it enters a strong field. This yields the ratio 2:45:37 for the relative populations of the  $F_1$  states when they leave the strong field. Figure (5c) shows the relative intensities that



would be expected for the  $\Delta F_1 = 0$  transitions after passing through the field. (3)

An Ammonia Beam in a Time Dependent Electric Field

The system composed of the upper and lower inversion state molecules is described by the wave function,

$$\Psi = c_I \Psi_I + c_{II} \Psi_{II} .$$

The matrix elements of the Hamiltonian  $H^{11}$  are

$$\langle \Psi_I | H^{11} | \Psi_I \rangle = E_0 - \sqrt{A^2 + \dots}$$

$$\langle \Psi_{II} | H^{11} | \Psi_{II} \rangle = E_0 + \sqrt{A^2 + \dots}$$

$$\langle \Psi_I | H^{11} | \Psi_{II} \rangle = \langle \Psi_{II} | H^{11} | \Psi_I \rangle^* = u E(t)$$

The time dependent Schrodinger equation yields the coupled equations,

$$i\hbar \dot{C}_{II} = (E_0 + A) C_{II} + uE(t) C_I \quad (14)$$

$$i\hbar \dot{C}_I = (E_0 - A) C_I + uE(t) C_{II} .$$

If it is assumed that  $E(t) = E \cos \omega t$ ,  $uE(t) \ll A$  and that the terms with  $\omega + \omega_0$  may be dropped. The above equations may be solved to yield:

$$C_{II} = \exp \left[ i \left( \frac{\omega}{2} - \frac{E_0}{2\hbar} \right) t \right] \left[ a e^{i\sqrt{R}t} - b e^{-i\sqrt{R}t} \right] \quad (15)$$

$$C_I = \frac{\hbar}{uE} \exp \left[ -i \left( \frac{\omega}{2} + \frac{E_0}{2\hbar} \right) t \right] \left[ (\Delta + \sqrt{R}) a \exp(-i\sqrt{R}t) + (\Delta - \sqrt{R}) b \exp(i\sqrt{R}t) \right] .$$

where

$$\Delta = \frac{\omega - \omega_0}{2} ,$$

$$\omega_0 = \frac{W_{II} - W_I}{\hbar} = \frac{2A}{\hbar} ,$$

$$\sqrt{R} = \sqrt{\Delta^2 + \left(\frac{uE}{\hbar}\right)^2} .$$

The constants  $a$  and  $b$  are subject to the initial conditions.

If at  $t = 0$   $C_{II}(0) = 0$  and  $C_I(0) = 1$ , then the equations;

$$C_{II}(t) = (i \cos \theta \sin \sqrt{R} t + \cos \sqrt{R} t) \exp i \left( \frac{\omega}{2} - \frac{E_0}{\hbar} \right) t$$

$$C_I(t) = (i \sin \theta \sin \sqrt{R} t) \exp - \left[ i \left( \frac{\omega}{2} + \frac{E_0}{\hbar} \right) t \right] , \quad (16)$$

are obtained, where  $\cos \theta = \Delta / \sqrt{R}$  and  $\sin \theta = uE / \hbar \sqrt{R}$ . The probability for a transition from  $\Psi_{II}$  to  $\Psi_I$  is given by,

$$P_{II \rightarrow I}(t) = |C_I(t)|^2 = \sin^2 \theta \sin^2 \sqrt{R} t . \quad (17)$$

#### An Ammonia Beam in Separated Oscillating Electric Fields

The transition probability will now be calculated for an ammonia beam which passes in succession through two time dependent electric fields of the same frequency, amplitude and phase. More general solutions for Equations (14) are,

$$C_{II}(t_0 + T) = \left\{ (i \cos \theta \sin \sqrt{RT} + \cos \sqrt{RT}) C_{II}(t_0) + i \sin \theta \sin \sqrt{RT} \right. \\ \left. \times \exp(i\omega t_0) C_I(t_0) \right\} \exp i \left( \frac{\omega}{2} - \frac{E_0}{\hbar} \right) T$$

$$C_I(t_0 + T) = \left\{ i \sin \theta \sin \sqrt{RT} \exp(-i\omega t) C_I(t_0) + (i \cos \theta \sin \sqrt{RT} \right. \\ \left. \cos \sqrt{RT}) C_{II}(t_0) \right\} \exp - i \left( \frac{\omega}{2} + \frac{E_0}{\hbar} \right) T . \quad (18)$$

These solutions are obtained at a time  $T$  for the molecules entering the field at a time  $t_0$  with  $C_{II}(t_0)$  and  $C_I(t_0)$ . For the beam entering a region of zero field we have, using the same initial conditions,

$$\begin{aligned} C_{II}(t_0 + T) &= \exp\left[-iE_{II}/\hbar T\right] C_{II}(t_0) \\ C_I(t_0 + T) &= \exp\left[-iE_I/\hbar T\right] C_I(t_0) \end{aligned} \quad (19)$$

If the beam enters the first field at  $t = 0$ , with  $C_I(0) = 0$ ,  $C_{II}(0) = 1$ , spends a time  $T$  there, then passes through a region of no field for a time  $3T$ , and finally passes through the second field, where it spends a time  $T$ , Equations (16), (19) and (18) may be applied in succession to yield,<sup>(4)</sup>

$$C_I(5T) = -2i \sin \theta \left\{ \cos \theta \sin^2 \sqrt{RT} \sin 3\Delta T - (1/2) \sin \sqrt{RT} \cos 3\Delta T \right\} \exp -i\left(\frac{\omega}{2} + \frac{E_0}{\hbar}\right) 5T \quad (20)$$

The transition probability from state  $\Psi_{II}$  to  $\Psi_I$  is given by,

$$P_{II \rightarrow I}(5T) = 4 \sin^2 \theta \sin^2 \sqrt{RT} (\cos 3\Delta T \cos \sqrt{RT} - \cos \theta \sin 3\Delta T \sin \sqrt{RT})^2 \quad (21)$$

Figure (6) is a plot of Equations (17) and (21). It is calculated for  $T = 10^{-4}$  sec. in (21), and  $t = 2 \times 10^{-4}$  sec. in (17), so that the time of interaction with the field is the same in both cases. The parameter  $\omega\hbar/\hbar$  is set at  $30 \times 10^4$  degrees/second, in both curves. The curves show the variation of the transition probability with the frequency of the time dependent fields. The separated oscillating fields thus produce a much narrower line width than does a single long field.

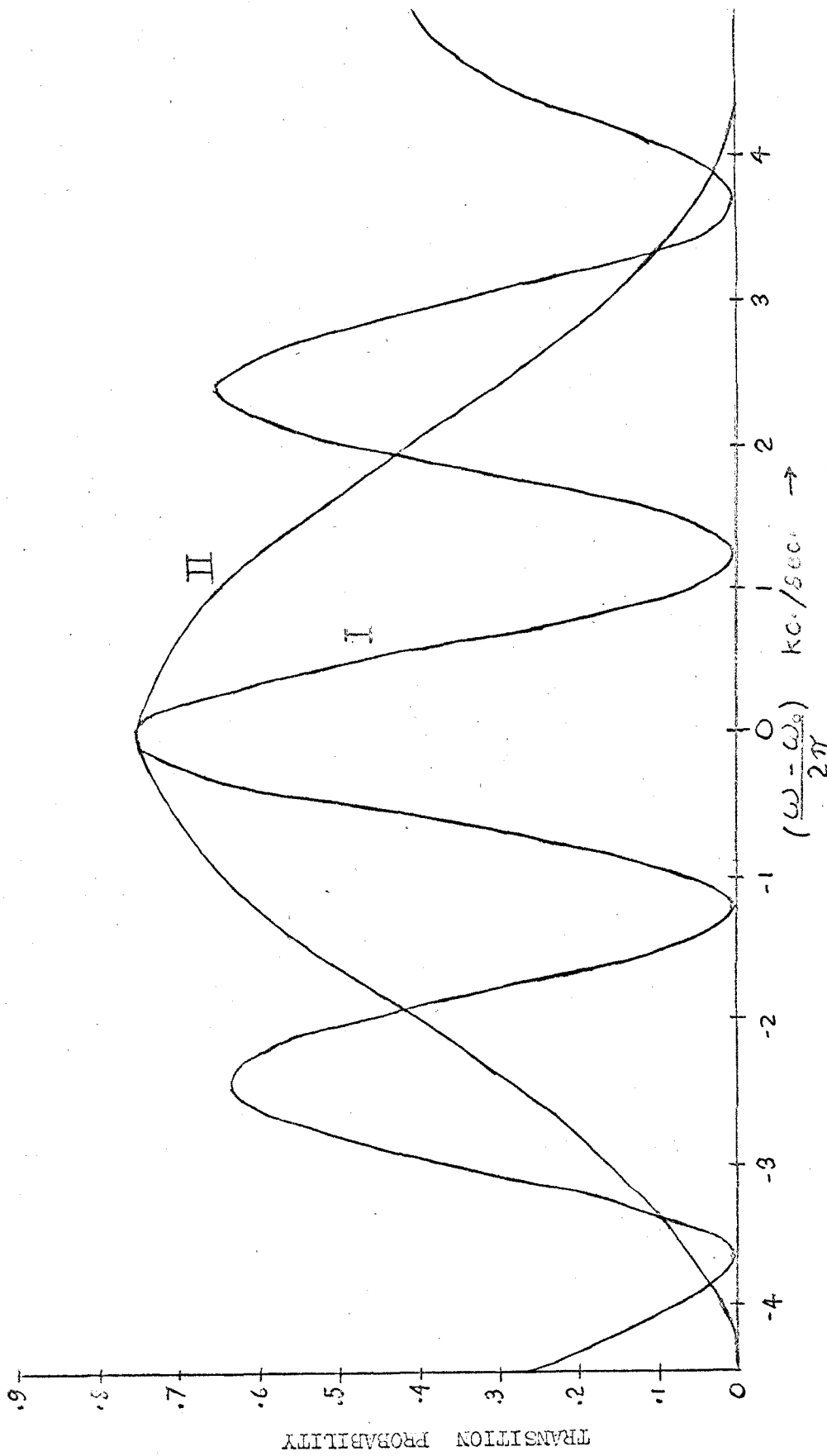


Fig. (6). Curve I indicates the transition probability for a beam of upper state ammonia molecules, passing through Ramsey separated oscillating fields. Curve II indicates the transition probability for the beam passing through a single field whose length is equal to the sum of the lengths of the two fields used for curve I.

The above calculations were made assuming a uniform velocity in the ammonia beam. If the effects of the velocity distribution are taken into account the widths of the transition probability curves will be increased. The velocity distribution will also have the effect of reducing the heights of the wings in the transition probability curve for the separated oscillating fields.

## CHAPTER III

### THEORY OF THE AMMONIA MASER

The inversion levels in a beam of ammonia molecules can be utilized to form a highly stable microwave oscillator in the following way. A beam of ammonia molecules is formed by effusion from a number of small parallel tubes. This beam is passed along the axis of a quadrupole electric field. This field has a strong gradient in the radial direction which removes the lower state molecules from the beam and focuses the upper state molecules. Leaving the state selectors the molecules, in the upper state, enter a resonant cavity where downward transitions, to the lower inversion state, are induced. When the number of molecules in the upper state reaches a certain critical number, the maser oscillates. When this critical number is exceeded, the beam alone can maintain a high enough energy density in the cavity to compensate for power lost through the coupling holes and in the cavity walls.

The beam current necessary for oscillation to start is obtained by equating the expression for the beam power to the expression for the power dissipated in the cavity. For a uniform velocity of the beam, this yields,

$$Nh\omega_0|c_I(t)|^2 = \omega_0 W/Q ,$$

where  $N$  is the number of upper state molecules entering the field,  $W$  is the energy stored in the cavity and is equal to  $\frac{1}{2} \epsilon E^2 V$ , where  $V$  is the volume of the cavity, and  $Q$  is the cavity  $Q$ .

If we substitute for the transition probability from Eq. (17) and assume  $\sin \sqrt{Rt} \approx \sqrt{Rt}$ , then we have at resonance,

$$1/N_c = 2Q (L/A) (u/v)^2 ,$$

where  $L$  is the cavity length,  $A$  is its cross-sectional area and  $v$  is the velocity of the beam. Thus we see, to minimize the starting current, the cavity should be long, small in cross-sectional area, and it should have a high  $Q$ .

The frequency of oscillation is determined by the reactance of the beam and by that of the cavity. If an ammonia molecule enters a cavity oscillating at a frequency  $\omega$ , the molecular dipole will start oscillating in phase with the field, and will continue to vibrate at its own frequency thereafter. By the time the molecule leaves the field, the average phase difference between the two frequencies will be  $(\omega - \omega_0) \frac{1}{2} T$  which is proportional to the reactance of the beam. The reactance of the cavity is, <sup>(5)</sup>  $2Q(\omega - \omega_c)/\omega_c$ , where  $\omega_c$  is the natural frequency of the cavity. For resonance the sum of these two reactances must equal zero, i.e.:

$$\omega - \omega_0 \approx (\omega - \omega_c) 4Q/T\omega .$$

The expression  $4Q/T\omega$  represents an effective  $Q$  for the molecular

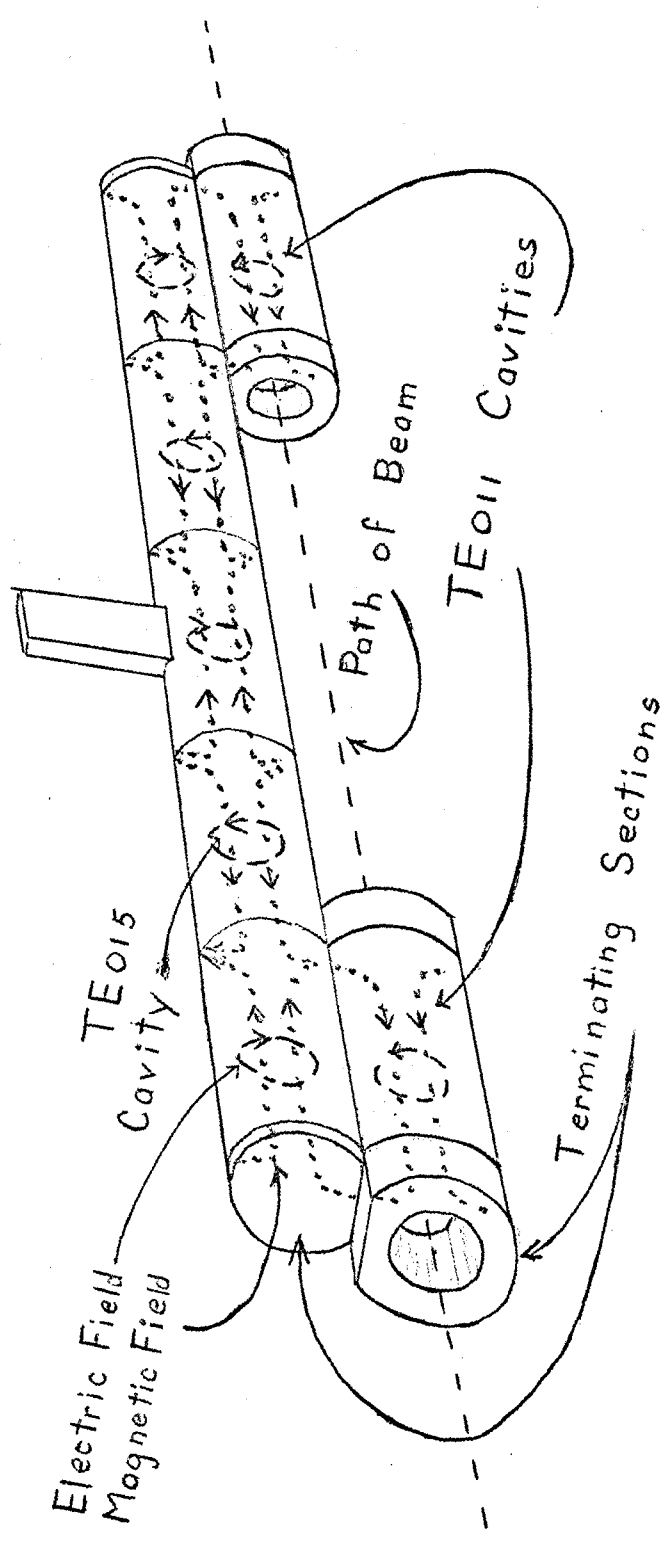


Fig. (7). TE cavity system showing field lines as would be seen in the longitudinal cross-section.



oscillator, with a band width of  $1/T$  cycles per second. This roughly corresponds to the frequency range over which the maser can be tuned.

It is shown in the above discussion that the width of the ammonia maser line can be decreased by increasing the length of the cavity. There are, however, practical limitations to the amount the length may be increased. The mode of oscillation of the cavity must be such that there is no more than half a wavelength of the field in the direction of the beam. This prevents the use of single cavities in modes other than  $TE_{lml}$  and  $TM_{lml}$ , or  $TM_{lmo}$  and  $TE_{lmo}$ .

A serious disadvantage of long cavities is the Doppler broadening of the line which occurs due to the difference in time it takes for the maser power, from different parts of the cavity, to reach the coupling to the measuring devices.

To overcome the difficulties in reducing the line width of the maser, a cavity system simulating the effects of Ramsey separated fields was constructed.<sup>(4)</sup> There is no exact solution to the problem involving the passage of the beam through this Ramsey separated field cavity system. The theory previously worked out for the Ramsey separated fields should however give approximately the correct results. The transition probability curves shown in Fig. (6) were calculated for a single resonant frequency of the beam. As was shown in the section on hyperfine structure the actual transitions occur between hyperfine energy levels. For  $J = 3$   $K = 3$   $\Delta F_1 = 0$  transitions, the two lines  $F_1 = 3$  and 4, are the

most intense, while the third may be neglected. The two lines and their frequency separation are shown in figure (5c). In Figure (8) the transition probability curves calculated from Equation (21), for each hyperfine line are shown. They are weighted by the relative populations that would be found as shown in Fig 5(c). The amplitudes of the two lines are added to show the resultant line shape expected when maser action occurs with both transition lines present.

120924

**UNIVERSITY OF WINDSOR LIBRARY**

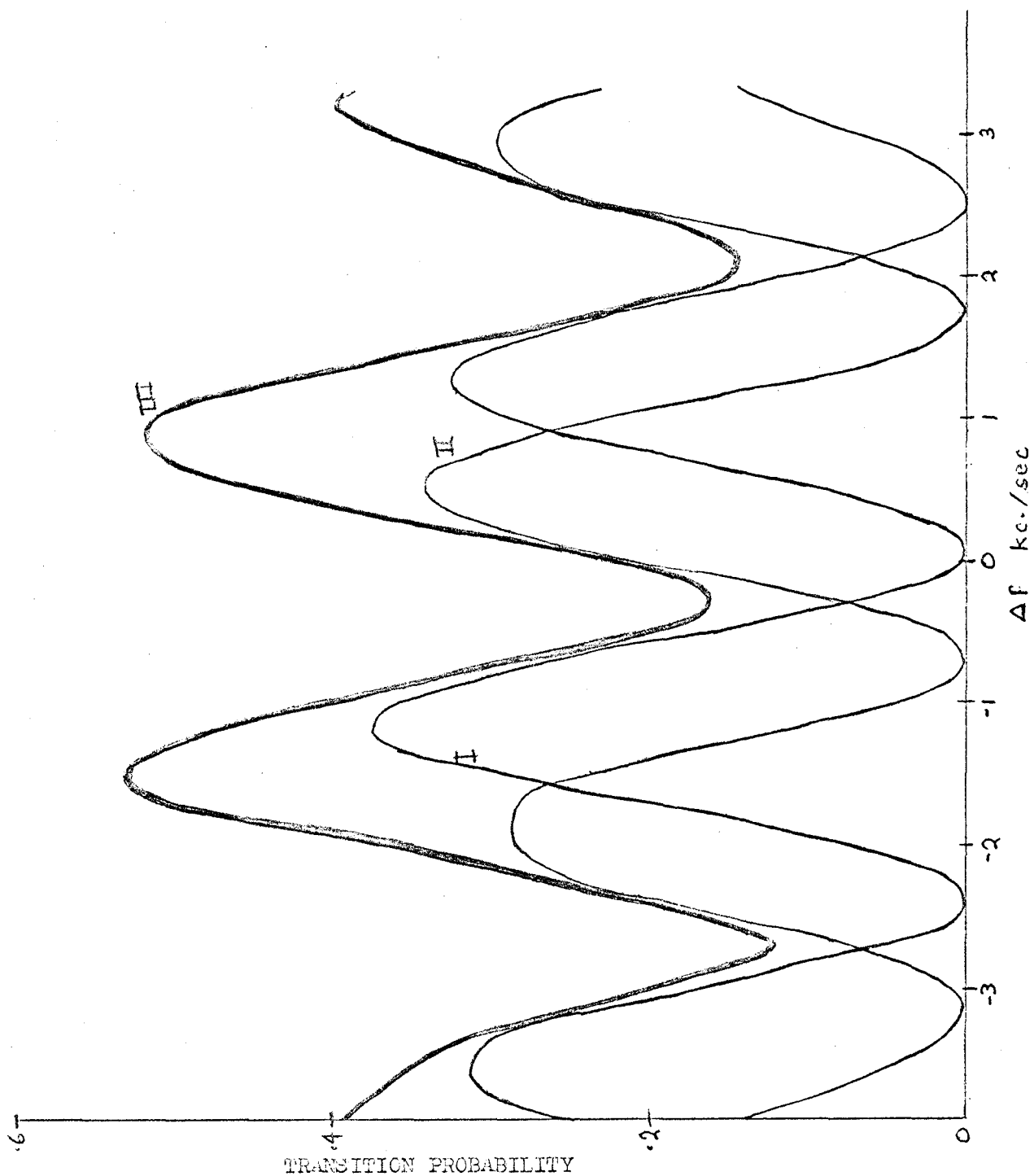


Fig.(3). Curve I is the transition probability for the  $F_1 = 3$  component of the hyperfine structure. Curve II is that for the  $F_1 = 4$  component. Curve III is the superposition of the two components.  $\Delta f$  is the difference in frequency from that which would occur if there were no hyperfine structure.

## CHAPTER IV

### APPARATUS

#### Introduction

The physical configuration of the apparatus used is shown in Fig. (9). Ammonia from the storage tank J, was leaked through two valves, I, to sources, E. The pressure behind the sources was measured by Pirani gauges, H. After effusing from the sources the ammonia molecules passed through the state selectors, D, then through the cavity system A, B, C. Output power from the maser passed through waveguide, L. Shutter, M, prevented the beams from passing through both cavities, A and B. The entire system of cavities, focusers, and sources was enclosed by the vacuum system, K, with the liquid air traps, G and F. The traps are semi-cylindrical so that they partially enclose the state selectors. The remainder of the apparatus consists of the electronics used to measure the frequency and amplitude of the maser signal. A more detailed description of the various components described above shall now be given.

#### Sources

The sources consisted of circular bundles of fine tubes. The diameter of each tube was .06 mm. and the length was .5 mm. About 320 such tubes formed a circular source of .7 mm. diameter.

The sources were prepared in the following manner. A

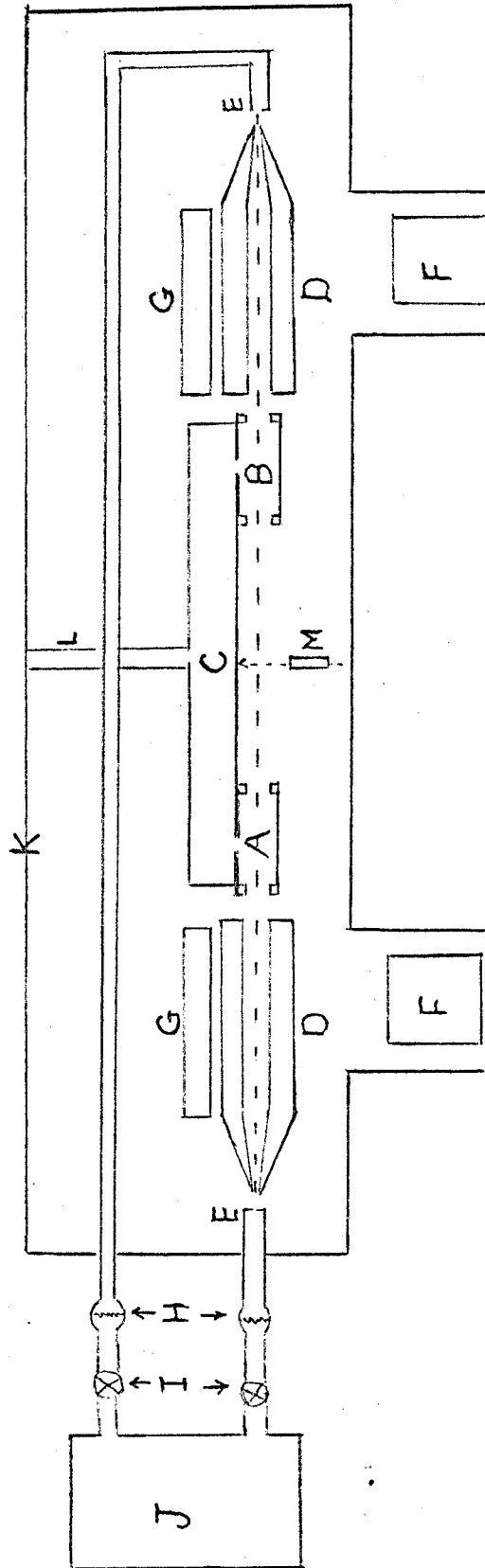


Fig. (9). Schematic diagram indicating the physical arrangement of the maser apparatus. A, B and C, cavity system, D focussers, E sources, F liquid air baffles, G liquid air traps, H Pirani gauges, I leak valves, J ammonia cell and K vacuum chamber.

bundle of number 46 magnet wire was impregnated with epoxy resin. Care was taken to insure that each strand of wire was straight and parallel to the axis of the bundle. When the epoxy had hardened the bundle was placed along the axis of a cylindrical form which was also filled with epoxy. From the rod, so formed, cross-sectional wafers about 1 mm. thick were cut. These wafers were polished until they were of the right thickness and until the cross-section of each of the wires at the center of the bundle was visible under a microscope. The copper was then removed electrolytically. This bundle of tubes formed an efficient source for the ammonia beam.

#### State Selectors

The state selectors are shown in Fig. (10). They consist of stainless steel rods mounted on teflon stands. They are constructed according to a design first used by Helmer<sup>(6)</sup>. The shape of the focuser is such, that it is not only highly effective in removing the lower inversion state molecules, but collimates the remaining upper state molecules as well.

#### Cavity System

The cavity system, shown in Figure (7), utilises a TE mode of oscillation. A similar system has been previously used,<sup>(7)</sup> employing a TM mode. The TE system has the advantage of offering a larger aperture for the beam to pass through.

The cavity system designed in this manner affects the molecular beam in a manner analogous to Ramsey separated oscillating fields. Cavities A and B, which produce the separated

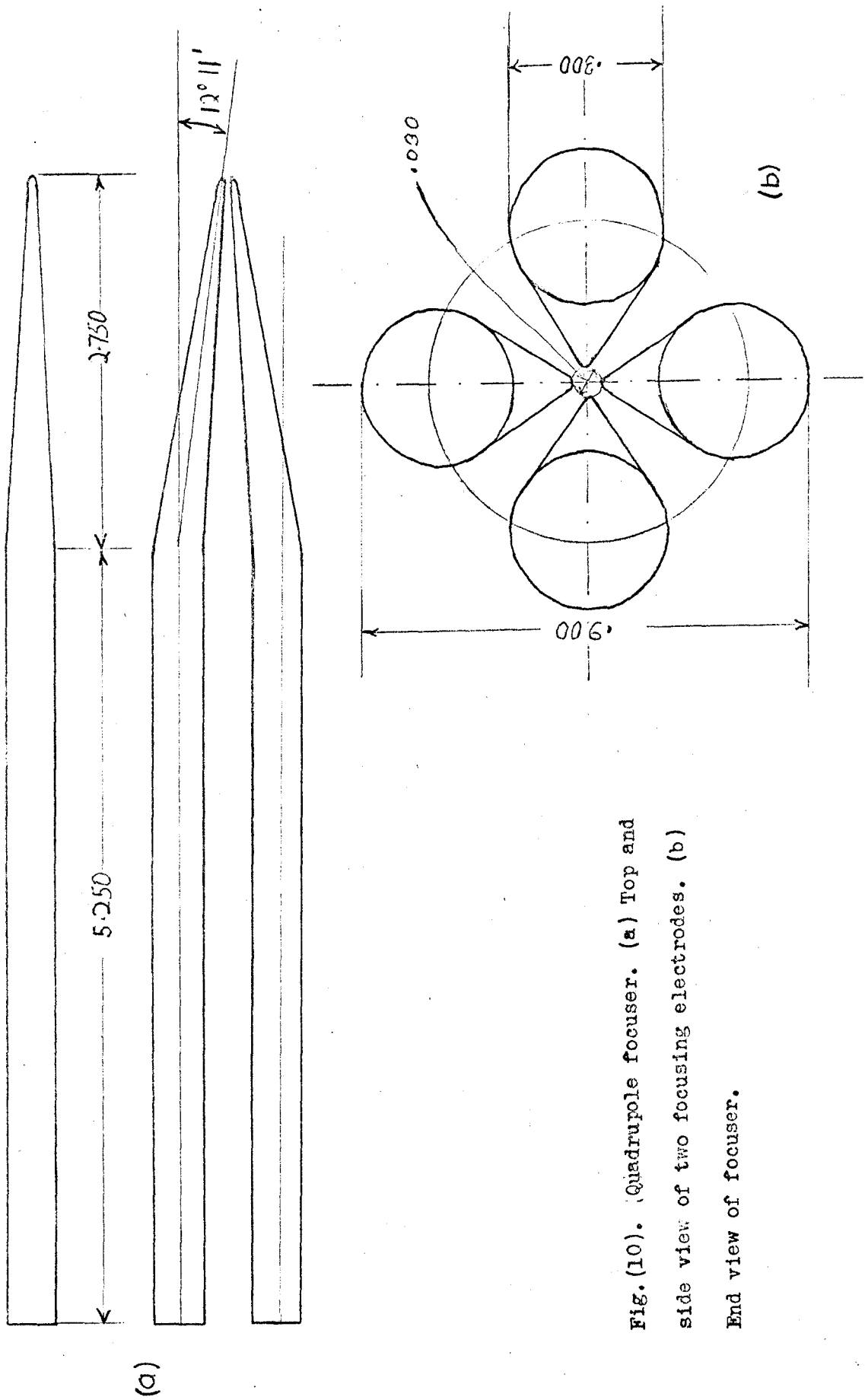


FIG. (10). Quadrupole focuser. (a) Top and side view of two focusing electrodes. (b) End view of focuser.

fields, are tightly coupled to cavity C, which determines the frequency and phase of A and B. Cavity C is also loosely coupled to the detection system.

The three cavities were constructed of brass. The ends of cavity C were terminated by means of brass plates. Cavities, A and B, through which the beam passed, were terminated by means of short cylindrical tubes whose inner diameters were smaller than that of the small cavities. For a given length, and the modes of oscillation used, the resonant frequency of the three cavities varied inversely with their radius. This allowed us to increase their frequency by plating copper to their inner surfaces and to decrease their frequency by polishing their inner surface. It was by this means that the cavities were tuned to the desired resonant frequency.

The resonant frequency of the  $TE_{015}$  cavity was measured using the apparatus shown in Figure (11). The correct mode of oscillation was determined by inserting plungers in the ends of the cavity and observing the corresponding changes in frequency of the various modes. Once the proper mode was found the frequency was measured as follows. Part of the frequency modulated output of the klystron was mixed with the 12th harmonic of a 2000 mc. reference. The I.F. thus obtained was passed through a narrow band radar receiver whose output was fed to the Y axis of the oscilloscope. This produced a marker whose frequency depended on the tuning of the receiver. The receiver was then tuned until the marker coincided with the resonant mode of the cavity.



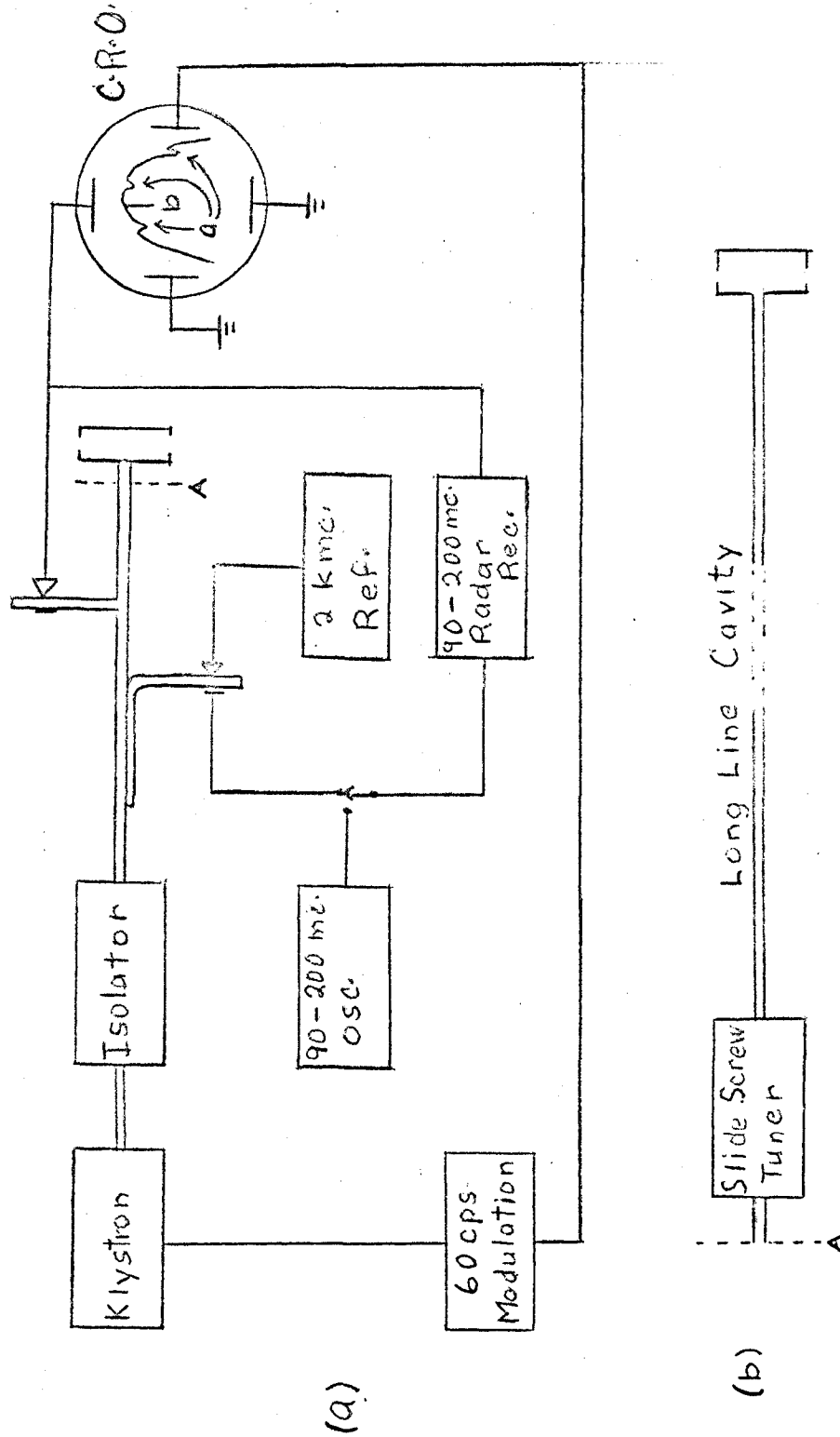


Fig. (11). (a) The experimental arrangement used to measure the resonant frequencies of a weakly coupled cavity. The display on the scope indicates, a, the cavity modes of oscillation, b, the pip due to the radar receiver.

(b) The modification necessary to measure the frequency of a strongly coupled cavity.

This enabled us to measure the frequency of the cavity to within .5 mc.

To measure the frequency of the  $TE_{011}$  cavities, a method proposed by R. Alvarez<sup>(8)</sup> was used. With this method a slide screw tuner and a long line cavity, consisting of twenty feet of waveguide, was placed between the cavity under investigation and the detector. With this arrangement the modes of oscillation of the long line cavity fall at equal frequency intervals. However, near the resonant frequency of the small cavity this spacing is changed. The frequency of the cavity is determined by adjusting the slide screw tuner until the spacings become symmetrical about a central mode. The frequency of this mode is the cavity frequency.

#### Electronics

The purpose of the electronics used in this experiment was to measure the power and the frequency of the maser signals. Figure (12) is a block diagram of the electronics used.

The signal from the maser was passed through a K band waveguide, through a ferrite isolator and into the H arm of a magic T. This signal is mixed with the local oscillator signal (23,930 mc.) appearing in the E arm, by crystals in the two side arms. The difference frequency from the side arms is fed into a balanced pre-amplifier. Leaving the balanced mixer the signal is amplified and mixed with a 60 mc. standard, which yields the second I.F. at approximately 120 kc. This signal is then passed through a narrow band amplifier and divided into two parts. The

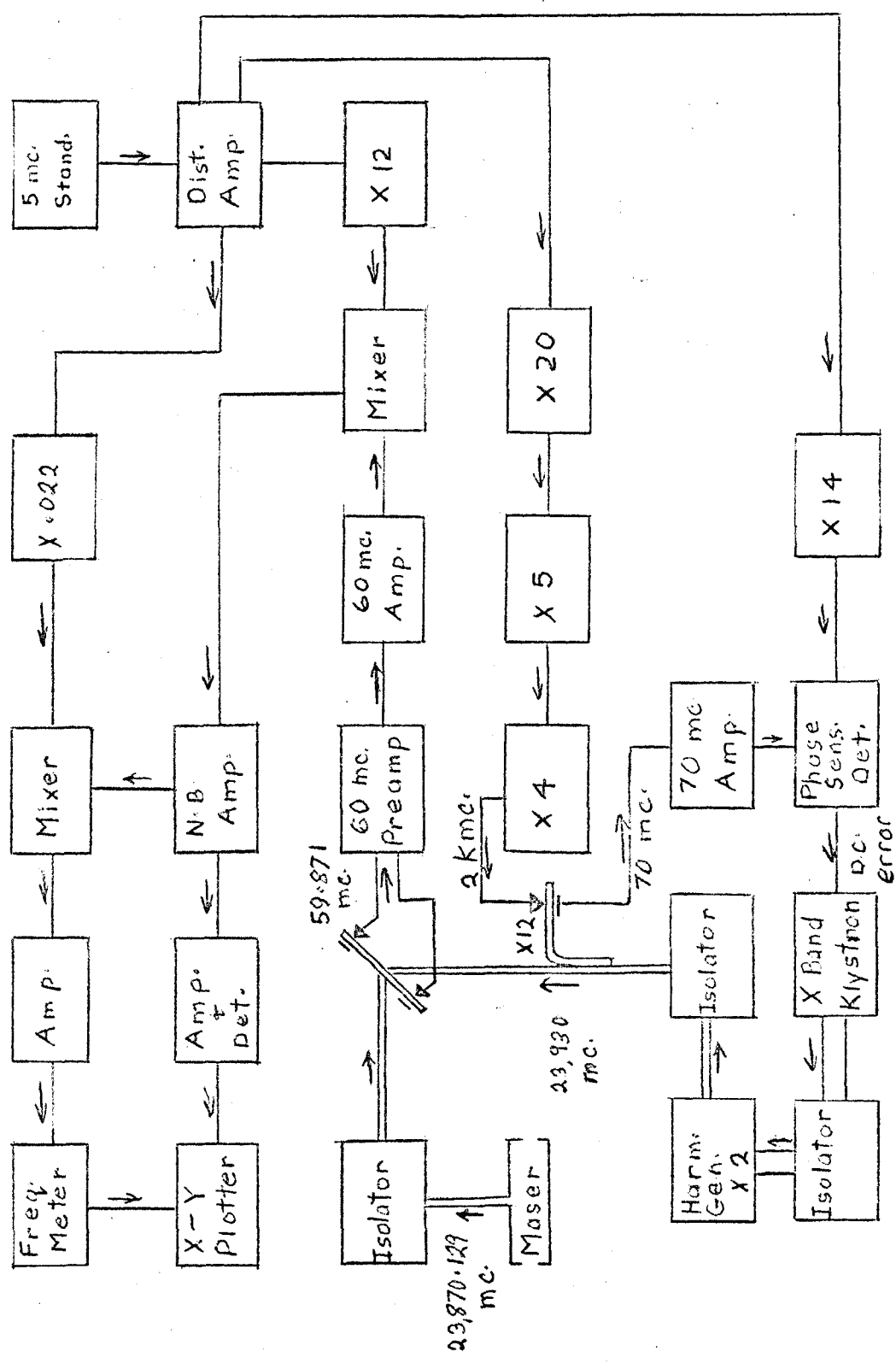


Fig. (12). Block diagram of maser electronics

first part is detected and fed to the Y axis of an X-Y plotter. The second part is mixed with the signal from a 110 kc. reference, the difference frequency is passed through a frequency meter with a recorder output in the form of a D.C. voltage proportional to the input frequency. This voltage is fed to the X axis of the X-Y plotter. Thus as the maser is tuned through its range of oscillation, the recorder traces out the curve of the amplitude of its signal against the frequency.

The primary frequency standard used in this experiment was a 5 mc. temperature controlled crystal oscillator. This primary signal was fed into a distribution amplifier, whose outputs were multiplied to yield the necessary reference frequencies for the mixers and klystron stabilization.

The 23930 mc. local oscillator signal was obtained in the following manner. The signal from an X band klystron oscillating at 11,965 mc. was passed through a ferrite isolator into a harmonic generator. The second harmonic (23,930 mc.) was picked up by the K band system, fed through another isolator and then went to the magic T. Part of this signal was removed using a directional coupler. This was mixed with the 12th harmonic of a 2,000 mc. reference. The I.F. of 70 mc. was amplified and fed along with a 70 mc. reference signal into a phase sensitive detector, which applied a correction voltage to the reflector of the klystron as the I.F. changed.

### The Vacuum and Ammonia Supply Systems

The main vacuum chamber was constructed of stainless steel, with glass ports for viewing the components inside. The vacuum was attained by means of two four inch diffusion pumps backed by a two inch pump and a mechanical pump. There were liquid air traps placed above the two diffusion pumps. Liquid air traps also partially enclosed the state selectors to capture the lower state molecules. At liquid air temperature the vapour pressure of ammonia is considerably less than  $10^{-6}$  mm. so the liquid air traps were quite efficient in removing the ammonia molecules from the system. With liquid air in the traps the pressure in the tank was  $10^{-7}$  mm. in absence of the beams, and it was  $10^{-6}$  mm. with the beams. At this pressure the mean free path of the ammonia molecules was several meters.

The ammonia was kept in a large cell outside the vacuum tank. It was purified by distillation using liquid air. The cell pressure was approximately equal to that of the atmosphere. From the cell ammonia was leaked through copper tubing to the sources. The pressure on the high pressure side of the sources was from 1 to 10 mm. This pressure was monitored by means of Pirani gauges to estimate the beam flux.

## CHAPTER V

### EXPERIMENTATION AND RESULTS

The three cavities were tuned so that the system resonated at 23,865 mc. in air. The frequency of cavity C was measured to be 23,865.3 mc. with the coupling holes for cavities A and B shorted. It was measured to be, 23,864.8 mc. with only cavity A coupled to it, and 23,864.9 mc, with only cavity B coupled. When the system was placed in a vacuum the frequency was 23,874 mc. The cavity system frequency was then swept through the resonant frequency. Great care was taken in assembling the maser, to be sure that the beams passed down the axis of the system.

The maser was operated with beams entering both ends of the cavity system. Fig. (13) shows the experimental curves obtained for different values of beam pressure. The amplitude is plotted in arbitrary units and the frequency is in kc./sec. The absolute frequency was not measured since we were concerned only with the shape of the curve. The oscillations started when the pressure at both sources was 1.5 mm. the fields in the cavity system reached saturation at a source pressure of 9 mm. Throughout the experiment the focuser voltage was kept constant at 30 K.V.

Fig. (14) curve (I) is the line shape near saturation with the beam shutter open while curve (II) is the shape with the shutter closed. The frequency shift which occurred as the shutter was

opened and closed is also indicated in the Figure. When the system started to oscillate with the shutter closed on the low frequency side, the frequency of oscillation of the system with the shutter open was about 70 cycles higher, whereas on the high frequency side this difference in frequency was only about 25 cycles per sec., the transition between the two extremes being linear.

The experiment was repeated for different values of the coupling between the small cavities and the long one. Attempts were also made to improve the tuning of the three cavities. These attempts did not however change the results stated above.

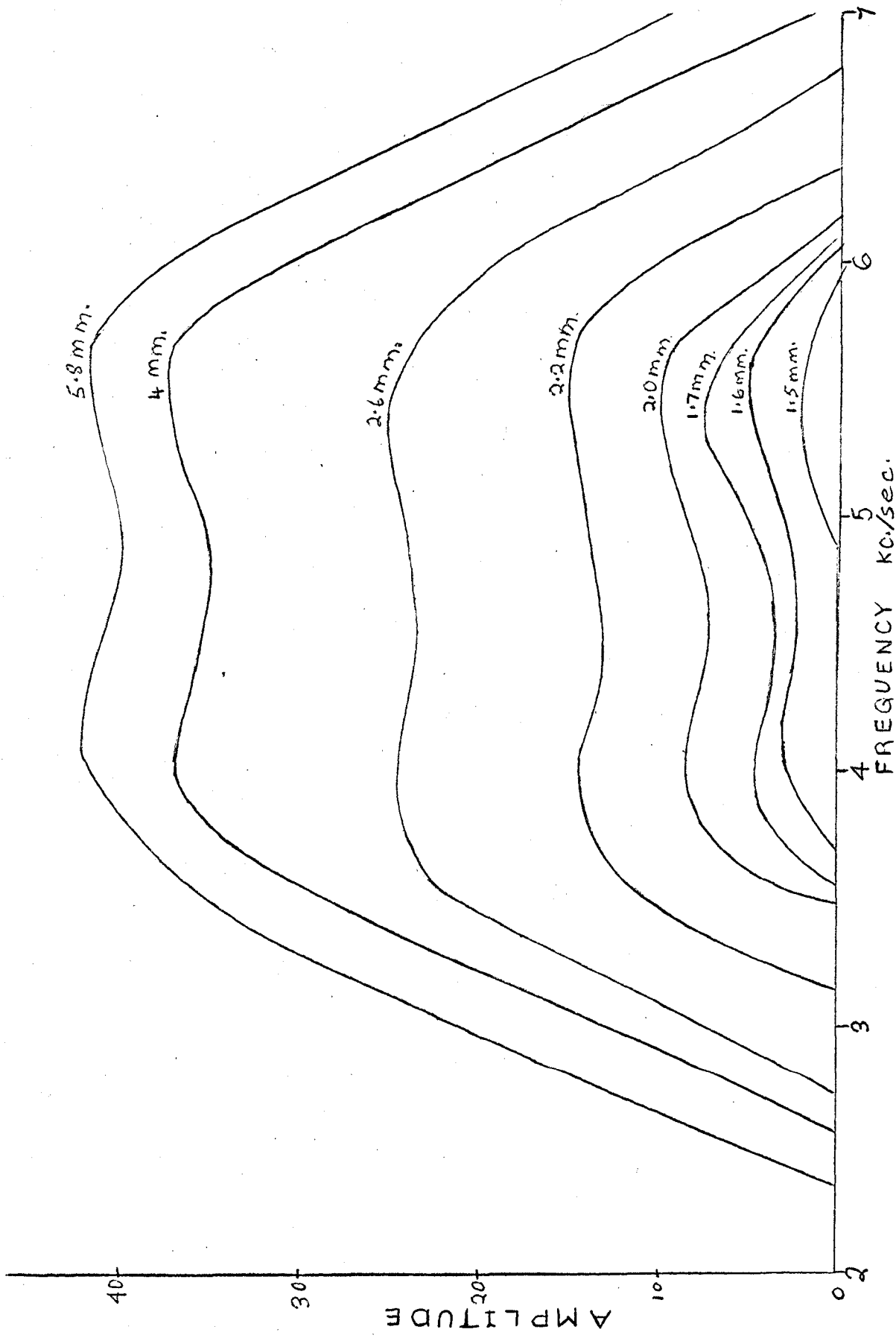


Fig. (13). The line shape of the maser for different beam pressures. The amplitude is plotted on an arbitrary scale.



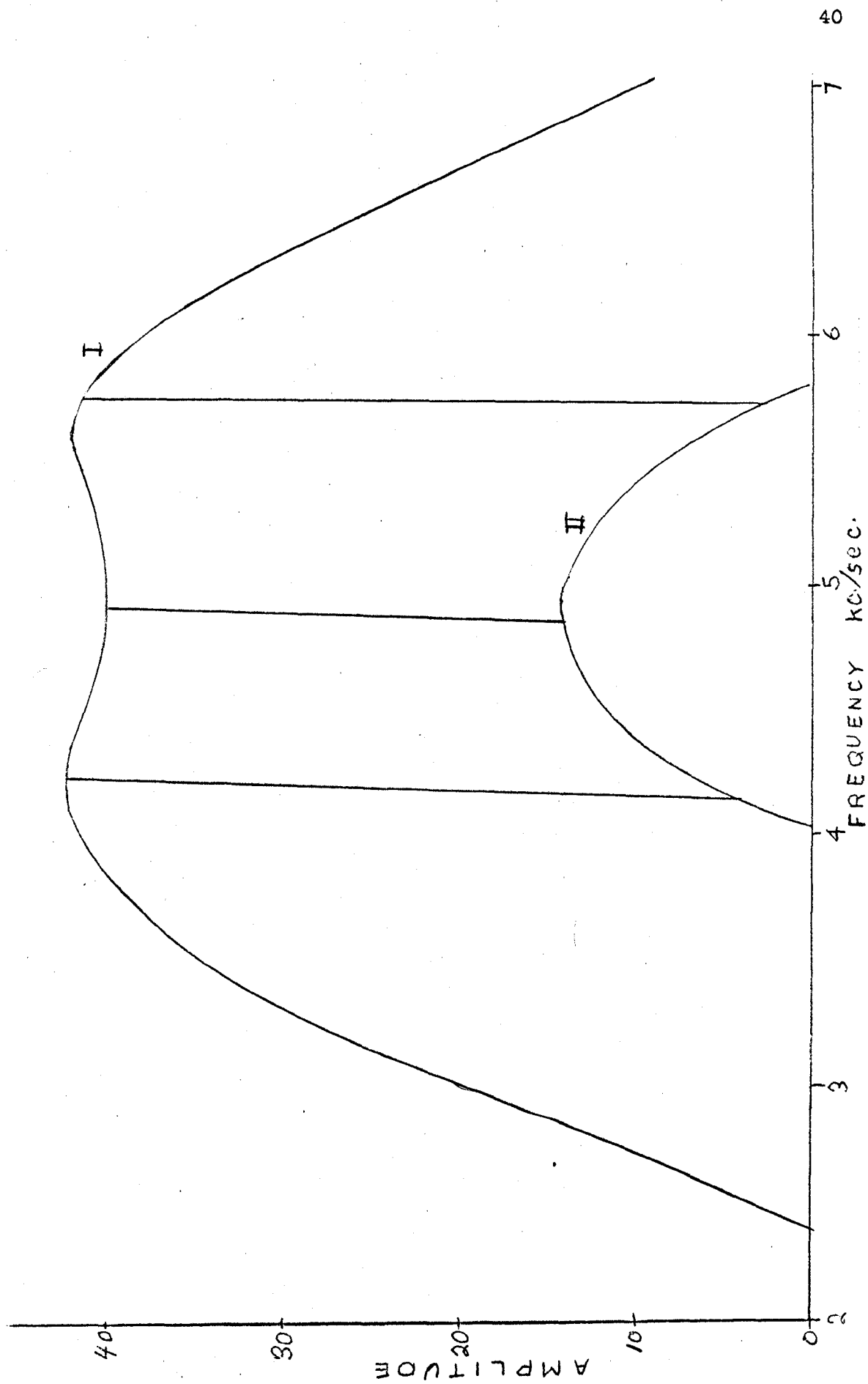


Fig. (14). Curve I indicates the line shape with the shutter open and the beam near saturation. Curve II indicates the shape for the shutter closed. The vertical lines indicate the difference in frequency of the two lines for the same value of cavity tuning.

## CHAPTER VI

### DISCUSSION

The line shape obtained in this experiment (Fig. 13) has two maxima separated, on the average, by 1.5 kc./sec. The reason for this shape is not definitely known, though two plausible explanations may be given.

Figure (14) shows the difference in frequency for the maser line with the shutters open and closed. At the centre of these lines there should be no difference in frequency for the two cases. This occurs because ~~the cavity pulling effect is absent in this case so that, formula,~~  $\omega = \omega_0 = \omega_c$  and there is no dependence on the number of molecules  $N$ . It has been shown that this formula for the cavity pulling holds near saturation when the natural frequency of the three cavities are the same.<sup>(7)</sup> Thus Fig. (14) indicates that the natural frequencies of the three cavities are not the same. If this is the case then there must exist a difference in phase in the electric fields of cavities A and B when the system is resonating at some frequency  $\omega$ . It has been shown by Gordon<sup>(2)</sup> that if the maser is operated with a cavity in which the mode of oscillation consists of more than one half-wavelength in the direction of the beam, the maser line observed will have two maxima, one on either side of the resonant frequency of the ammonia molecule. Such a cavity gives rise to a 180 degree phase shift in the field. Such a situation could exist in the cavity

we system used, and the line shape obtained could be due to the difference in phase of the cavities A and B.

The other possible explanation stems from the fact that  $J = 3 \quad K = 3$  inversion transition of ammonia has essentially two hyperfine components, of nearly the same intensity, denoted by  $F_1 = 3$  and 4. Fig. (8), which showed the superposition of the Ramsey transition probabilities for the two hyperfine lines, was calculated using the average velocity of the beam. The two peaks found by such a superposition are 2.3 kc. apart. If the velocity distribution were taken into account the peaks would be found somewhat closer together. There would also be an effect due to frequency pulling of the two lines. Fig. (12) indicates that the peak on the high frequency side of the line is greater in amplitude than the one on the low frequency side. This is opposite to what is expected when the relative intensity of the two hyperfine lines is considered. Thus it is impossible to conclude that the line shape is due to the hyperfine structure. It is more probable that it occurs because of a difference in phase between the two cavities.

To investigate the exact nature of the line shape obtained it would be necessary to construct a cavity system in which the three cavities could be tuned independantly while the maser was oscillating. Such a system would be very difficult to construct using the TE cavities, due to the fact that the currents in these cavities run around the circumference of the cavity. In the TM cavity, however, the currents run parallel to the axis of the cavity. This would

allow the cavity to be slit along its length and thus be tuned by means of squeezing the cavity. To construct such maser tuning, the whole vacuum system enclosing the maser would have had to be redesigned.

#### REFERENCES

1. C.H. Townes "Microwave Spectroscopy", McGraw-Hill Book Co. N. Y. (1955)
2. J. P. Gordon, H.J. Zeiger, and C.H. Townes, Phys. Rev. 99 1264, (1955)
3. K. Shimoda, J. Phys. Soc. Japan, 12, 1006, (1957)
4. N.F. Ramsey, "Molecular Beams," Oxford Press, (1963)
5. J.C. Helmer and F.B. Jacobus, J. Appl. Phys. 31, 458 (1960)
6. J.C. Helmer, Ph.D. Thesis, Stanford University
7. F. Holuj, H. Daams, and S.N. Kalra, J. Appl. Phys. 33, 2370 (1962)
8. R. Alvarez and J.P. Lindley, IEEE Transactions on Microwave Theory and Techniques, pg. 89 Jan. (1963)
9. D.V. Skobel'tsyn, "Soviet Maser Research", Consultants Bureau, N.Y. (1964)

VITA AUTORIS

1942 - born in Windsor, Ontario on March 7.

1960 - graduated from General Amherst Highschool, Amherstburg, Ontario.

1963 - Bachelor of Science in Physics, University of Windsor.

- Entered the Faculty of Graduate Studies, University of Windsor to proceed toward M.Sc. degree in Physics.

1964 - married.